

# Investigations with Zemax OpticStudio

ISAAC WOODARD<sup>1</sup>

<sup>1</sup>*Knight Campus Graduate Internship Program, University of Oregon, 1252 University of Oregon, Eugene OR 97403*

*\*isaac.j.woodard@gmail.com*

**Abstract:** Several basic optical systems were modeled using Zemax's OpticStudio software. For the first two systems a Keplerian and Galilean beam expander were optimized for beam quality, with the latter achieving a better  $M^2$  value. In the third system a lens for an SLR camera was designed for MTF targets both on and off axis with all targets being exceeded. The fourth system used OpticStudio's nonsequential mode to explore Young's double slit experiment and the effects of aperture shape on the diffraction pattern. Finally, three converging singlet lens of equal powers but different curvatures were created to compare the impact on aberrations. It was found that plano-convex and double convex designs produced similarly low aberrations, while the concave-convex design performed poorly.

## 1. Introduction

OpticStudio is a software made by Zemax which can be used to model many optical systems. There are many situations where it is useful to model an optical system before conducting an experiment or manufacturing a device. The model can predict optimal configuration and inform equipment needs. OpticStudio makes it easy to create visual models, provides numerous analysis tools, and offers methods for optimizing specific parameters of the system. Systems can be modeled in either sequential or nonsequential modes, with the former tracing rays through the system sequentially and the latter tracing rays through any order of components in the system [1]. There are many sample files which come installed with OpticStudio. These include files for nonsequential and sequential systems as well as sample code for working with the software's API.

The goal of this paper is to explore the features of OpticStudio by modeling four types of optical systems: afocal beam expanders, a composite lens system for an SLR camera, a nonsequential system to model Young's double slit experiment, and singlets assembled using OpticStudio's Application Programming Interface (API).

### 1.1. Afocal Beam Expanders

An afocal beam expander takes a collimated beam and transmits an expanded collimated beam. The term "afocal" comes from the object and image both lying at infinity [2]. There are two types of afocal beam expanders: Keplerian and Galilean. As illustrated in Fig. 1, a Keplerian beam expander is composed of two converging lenses, while a Galilean beam expander is composed of a diverging lens and a converging lens. For both types, the theoretical distance between the lenses should be the sum of their focal lengths.



Fig. 1. On the left is a Keplerian beam expander composed of two converging lenses. On the right is a Galilean beam expander composed of a diverging lens and a converging lens.

Characteristics of a good beam expander include correct magnification and collimation of the outgoing beam. The magnification is essentially defined by the focal lengths of the lenses and requires correct spacing of the lenses. The degree of collimation of the outgoing beam can be referred to as beam quality, though the term is somewhat ambiguous. This ambiguity is discussed by Siegman in his tutorial on measuring beam quality [3]. OpticStudio uses the method of second moments as outlined by Siegman for calculating the  $M^2$  value, which is a common measure of beam quality. A value of 1 indicates a beam with perfect collimation and cylindrical symmetry, with nonideal beams having values greater than 1.

When constructing either type of beam expander, the orientation of the two lenses isn't critical, but there are configurations which yield better beam quality (and fewer aberrations). Lens orientation refers to which surface of the lens faces the incoming beam.

In general a laser beam is modeled by a Gaussian. The propagation of the beam is characterized by its waist radius  $w_0$ , divergence angle  $\theta$  and wavelength  $\lambda$ . The waist radius and divergence angle can be related with  $\theta = \lambda/\pi w_0$ , so the Rayleigh range  $z_R$  can be calculated by [4],

$$z_R = \frac{\pi w_0^2}{\lambda} = \frac{\lambda}{\pi \theta^2}. \quad (1)$$

Modeling the laser propagation with ray traces can be a suitable substitute if the Rayleigh range of the laser is considered. If the propagation distance lies within the Rayleigh range, the beam can be modeled as a collimated bundle of rays; otherwise it should be modeled as a point source [4].

A 4x Keplerian and a 4x Galilean beam expander were modeled with the goal of optimizing the magnification and the beam quality of the transmitted beam. The lenses used are each planar on one side, so each combination of lens orientations is considered in optimizing the two systems.

## 1.2. SLR Camera

A single-lens reflex (SLR) camera offers the ability to look through the camera at the scene before capturing an image. This is done using a mirror or prism behind the main lens of the camera to direct the image to a viewing port. The mirror or prism is removed when the shutter is activated [5].

While commonly referred to as a single lens, the main lens for a camera is typically a series of several lenses. The series of lenses offers the ability to balance the aberrations of the individual lenses, giving a better quality image than a single lens could provide.

An important characteristic of the lens system is the F number. The F number is related to the effective focal length (EFL) and the entrance pupil diameter (EPD) by [6],

$$F/\# = \frac{EFL}{EPD}. \quad (2)$$

As a consequence, defining two of the three parameters in Eq. 2 determines the third.

The performance of a camera system is often described with the modulation transfer function (MTF). The MTF for an optical system defines the contrast the system can image at certain spatial frequencies [7]. OpticStudio measures the MTF using a sinusoidal target by default with spatial frequency in cycles/mm.

A composite lens system was modeled to image onto 35 mm film with specific MTF targets for optimization both on and off the optical axis. The targets were >50% at 30 cycles/mm and >20% at 50 cycles/mm on-axis, and >35% at 30 cycles/mm and >20% at 45 cycles/mm off-axis. The system was designed for imaging visible light by using the OpticStudio defaults of the F, d, and C Fraunhofer lines for the wavelengths in the system. Aberrations were also minimized with distortion kept below 1%.

### 1.3. Young's Double Slit

Young's double slit experiment is a classic demonstration of the wave properties of light. A monochromatic source is directed at a pair of slits so that a diffraction pattern appears on a screen behind the slits. The positions  $\Delta x_n$  of the bright spots, or peaks, in the pattern relative to the central spot can be predicted from the wavelength of the source  $\lambda$ , the distance from the slits to the screen  $L$ , and the slit spacing  $d$  [8]:

$$\Delta x_n = \frac{n\lambda L}{d}. \quad (3)$$

Young's double slit experiment can also be used to demonstrate the key features of nonsequential mode in OpticStudio such as sources, 3D objects, and detectors [8]. It might appear that sequential mode would work well to model slit diffraction since light is passing sequentially from the source to the slit and finally to the screen. While this is true, nonsequential mode works better for splitting and scattering the rays from the slits to allow the diffraction pattern to be observed [1].

Several slit diffraction systems with different slit configurations were modeled to compare the effects on the diffraction pattern. A double slit system with a slit spacing of 0.96 mm and a slit width of 0.01 mm was used as the standard. Two more double slit systems were created: one with a slit spacing of 0.48 mm and the other with a slit width of 0.005 mm. The fourth system had the same slit spacing and width as the standard but an additional 2 slits. From Eq. 3, we expect only a change in the slit spacing to affect the positions of the diffraction peaks.

### 1.4. Singlet Lenses with Zemax API

The building blocks of lens systems are individual lenses, also known as singlet lenses. Key properties of a singlet lens are the index of refraction of the material and the optical power. Optical power is the inverse of the focal length and can be predicted from the so-called lensmaker's equation if we assume a "thin" lens [9],

$$P_{lens} = \frac{n_{lens} - n_0}{n_0} \left( \frac{1}{R_1} - \frac{1}{R_2} \right). \quad (4)$$

The index of refraction of the surrounding medium is  $n_0$ , while the radius of curvature for the right surface along the optical axis is  $R_1$  and for the left surface is  $R_2$ . The sign convention is positive for curvature bending right along the optical axis.

There are in principle an infinite number of ways to shape a lens to achieve a certain power. Certain pairs of curvatures for the lens faces might be expected to lead to different amounts of aberrations, though. Two common ways to shape a lens are to leave one face flat or shape both faces to have equal curvatures.

The need to analyze a large number of similar optical systems indicates OpticStudio's API might be a useful tool for improving efficiency. It is possible to create or modify optical systems using the API depending on the mode the user chooses. One of the modes creates a standalone application which opens a new instance of OpticStudio and offers full control over the optical system. OpticStudio offers convenient support for connecting to the API with C#, C++, Python and MATLAB.

Using OpticStudio's API, three singlet lenses with equal powers but different curvatures on each face were modeled to compare the impacts on aberrations at the foci. The first singlet was plano-convex, the second was double convex with equal curvatures on each face, and the third was convex on one face and concave on the other with the magnitude of the convex radius being half that of the concave radius.

## 2. Methods

### 2.1. Afocal Beam Expanders

Both a Keplerian and a Galilean beam expander were modeled. Each was composed of two lenses with the input beam modeled after a Thorlabs HeNe HNL100LB laser. Since input and output beams of a beam expander are ideally collimated the afocal setting was used for the environment [2]. This changed the object and image heights to angular measurements.

The Keplerian expander was modeled with a Thorlabs LA1252 and LA1251 lens, having focal lengths of approximately 25 mm and 100 mm respectively. The Galilean expander was modeled with a Thorlabs LC1054 and LA1251 lens, with the LC1054 having a focal length of approximately -25 mm. Lenses were inserted into the models from the Zemax lens catalog.

Four different configurations were made for each system (with one file for each system) to model every possible combination of normal lens orientations while keeping the lens order the same. In practice, this required using the CRVT operand in the MC editor to set the lens curvatures for each combination. The thickness of the air between the lenses was set as a variable to allow for optimization of the distance between them.

Merit functions for each system were set up with operands for the outgoing spot size (REAY) and the beam quality (POPD) at the image surface. While optimizing the spot size and beam quality, the wavefront optimization function was used to reduce aberrations. Desired expansion for the expanders was 4x, so the REAY operand was given a target of 10 mm for an aperture value of 5 mm. The POPD operand was given a target of 1 corresponding to ideal beam quality. Beam quality was considered a more important factor than spot size so it was given a higher weight in the merit function. Configurations with the best beam quality for each system are shown in Fig. 2.

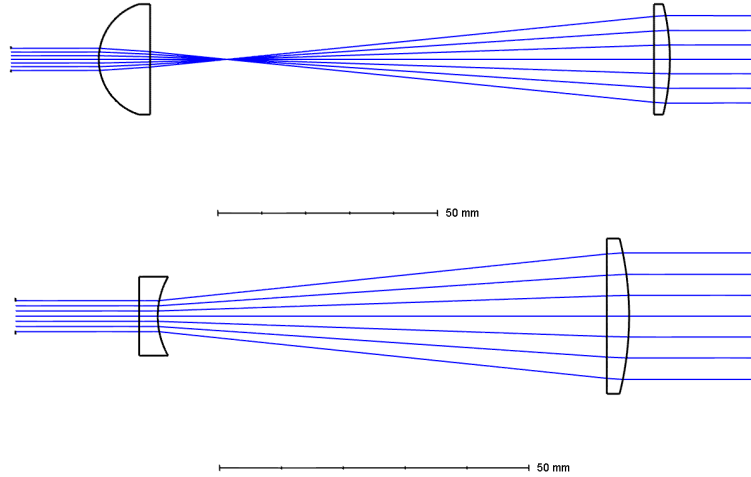


Fig. 2. 2D cross sections of the beam expanders modeled in OpticStudio. On the top is the optimal lens orientation for the Keplerian expander. On the bottom is the optimal lens orientation for the Galilean expander.

The wavelength of the laser was 632.8 nm and the divergence angle was 1.2 mrad [10]. This gave a Rayleigh range of 140 mm from Eq. 1. Lens separation for the longer Keplerian system was just within the Rayleigh range, making a collimated bundle of incoming rays a suitable model for the laser beam.

## 2.2. SLR Camera

An SLR camera lens was modeled by modifying OpticStudio's "Double Gauss 28 degree field" sample file. A cross section of the lens system after the final optimization is shown in Fig. 3.

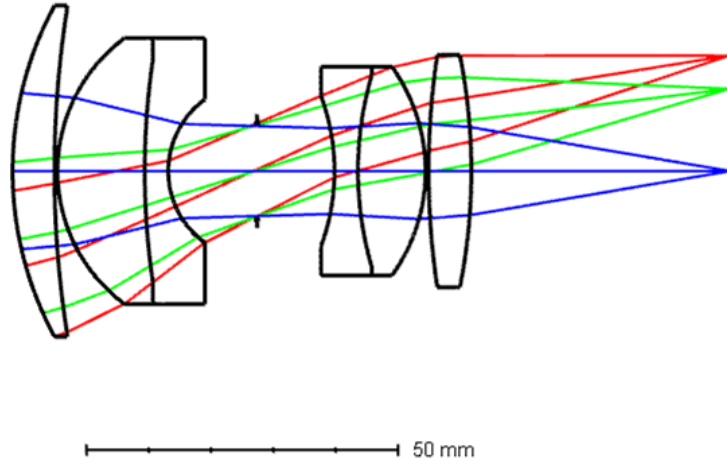


Fig. 3. 2D cross section of the SLR lens system. Rays at incident angles of 0, 10 and 14 degrees are being imaged through the system. The ray colors correspond to the three wavelengths of visible light in the system, though the individual coloration is arbitrary.

Environment wavelengths were left on the default preset for visible light (F, d and C Fraunhofer lines). An F number solve of was added to the radius of the final lens surface. Using Eq. 2, the entrance pupil diameter was set to 25.0 mm to give an effective focal length of 75.0 mm. The Quick Focus feature was then used to bring the image plane into focus in the new system. This brought the image plane to a back focal distance of 41.5 mm (from the surface of the last lens). The thickness of the last surface before the image was then set to fixed to avoid changing the back focal distance.

The next step was performing the optimization of the system to minimize aberrations and obtain the target MTF values. The merit function was set to minimize wavefront error with glass boundary values of 2 to 12 mm and a minimum edge thickness of 2 mm. Distortion was set to a maximum value of 0.9 % using the DIMX operand.

For the first optimization attempt, operands for optimizing the MTF were added before running the optimization. There are several operands available in OpticStudio for optimizing the MTF. The MTFA operand takes the average of the MTF in the tangential and sagittal directions, making it suitable for off-axis optimization. The MTFT and MTFS operands uses the value of either the tangential or sagittal MTF, respectively, making them suitable for on-axis optimization where there is radial symmetry. MTFS operands were added to the on-axis ray for the two on-axis MTF targets and MTFA operands were added to the most extreme off-axis ray for the off-axis MTF targets. Using this setup for the merit function, optimization failed to reach target MTF values.

On the second attempt, additional surface parameters were set to variable: the radius of surfaces 4 and 8 and the thickness of surface 1. The merit function was again set to optimize wavefront error with the previous glass boundary values, but this time optimization was performed without adding the MTF operands. This produced a lens configuration with the desired MTF targets.

## 2.3. Young's Double Slit

A tutorial from Zemax's knowledgebase was used to set up the software for modeling Young's double slit experiment [8]. It provided a sample file containing a source diffractive object and a

rectangular detector object. The source wavelength was 584 nm and the distance from the slits to the detector was 13.7 m. OpticStudio's default double slit aperture file came preloaded on the source diffractive object. The double slit aperture had a slit spacing of 0.96 mm, a slit height of 1 mm, and a slit width of 0.01 mm. Shown in Fig. 4 is a schematic of the system.

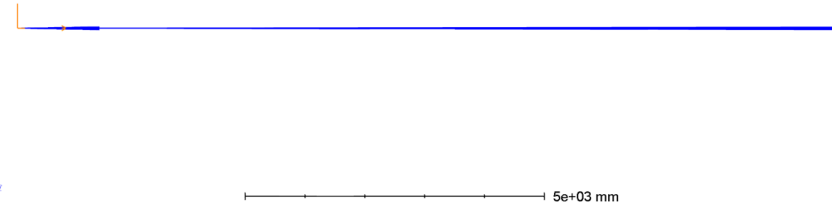


Fig. 4. Topdown view of the source and detector system viewed with OpticStudio's NSC 3D layout tool.

One of the important differences from sequential modeling was the need to specify sampling parameters for the ray trace. The number of rays to trace was left unchanged from the sample file but the X and Y pixel dimensions of the detector were increased from 100 to 400. This greatly improved the visibility of the diffraction pattern.

A diffraction pattern was collected for the default aperture file. Three additional aperture files were created as described in the Introduction. Diffraction patterns were collected from the modified aperture files and compared to the pattern from the default aperture.

#### 2.4. Singlet Lenses with Zemax API

Three lenses were created using OpticStudio's API. Visual Studio was used as the integrated development environment (IDE) as recommended in Zemax's knowledgebase tutorial "Using ZOS-API with C# and C++: what to install" [11]. The workloads ".NET desktop development" and "Universal Windows Platform development" were installed to allow Visual Studio to connect with OpticStudio using the C# programming language.

So-called "boilerplate" code to create a lens file in OpticStudio was generated by selecting the Standalone Application option for C#. Code from the sample file "CSharpStandalone\_01\_new\_file\_and\_quickfocus.cs" was then added to make a working example of a singlet lens. To create the lens file, the code was run in Visual Studio using Build > Build Solution and then Debug > Start Without Debugging. A new instance of OpticStudio was opened with the program and the OpticStudio file was saved after creating the lens.

The program was ran and modified three times to create the different lenses. The plano-convex lens had a convex radius of 100 mm, the double convex lens had a convex radius of 200 mm on each side, and the concave-convex lens had a concave radius of 100 mm and a convex radius of 50 mm. EPD for each system was 40.0 mm with a field along the optical axis and a second field at 5°. Environment wavelength was set to 588 nm and the material of the lenses was N-BK7 with a thickness of 10 mm for each lens.

### 3. Results & Analysis

#### 3.1. Afocal Beam Expanders

The lens separation, expanded radius, and beam quality for each pair of lens orientations in the Keplerian and Galilean systems is summarized in Table 1. We can see that the optimal configuration in terms of beam quality for the Keplerian system was the C-F lens orientation, while for the Galilean system it was F-F. We also see that the optimal beam quality configurations

were not the same as the optimal configurations for beam expansion. For the desired 4x expansion, the optimal configurations were the F-C lens orientation for the Keplerian and the C-C orientation for the Galilean.

Orientation	Keplerian				Galilean			
	C-C	C-F	F-C	F-F	C-C	C-F	F-C	F-F
Separation (mm)	115.5	114.7	122.7	122.0	70.81	70.26	73.21	72.62
Exit Radius (mm)	9.852	9.883	10.038	10.074	9.994	10.045	10.134	10.18
Beam Quality	3.364	1.685	3.511	2.329	3.313	1.325	2.939	1.001

Table 1. Summary of key measurements for all lens orientations of both beam expanders. The orientation denotes whether the curved (C) or flat (F) surface of the first and second lens faces the incident beam. The separation refers to the lens separation and the exit radius is the radius of the expanded beam.

Shown in Fig. 5 and Fig. 6 are the spot diagrams and ray fans for the optimal beam quality configurations of the Keplerian and Galilean systems, respectively. The cubic shape of the ray fans for both systems indicates the presence of spherical aberrations, while the tilt from the x-axis indicates a degree of defocus [12]. Spherical aberrations can also be clearly seen in the spot diagrams from the uneven spacing between each ring of spots. This is due to rays receiving different degrees of focus depending on their distance from the optical axis [12]. Between the two systems, the Galilean has a much smaller disc size. This likely corresponds to its lower beam quality value.

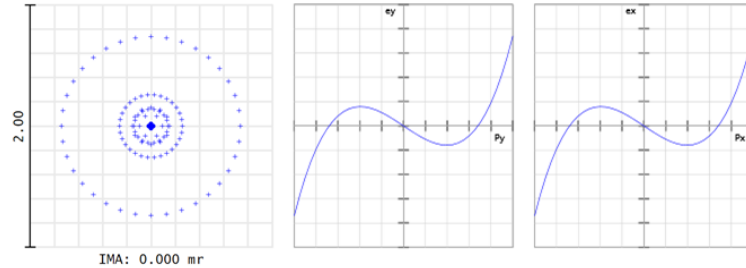


Fig. 5. Spot diagram and ray fan diagrams for the Keplerian beam expander with optimal lens orientation (C-F). The units of the spot diagram are milliradians.

### 3.2. SLR Camera

The main goal of the optimization for the SLR system was to reach MTF values at specific spatial frequencies. Shown in Fig. 7 are the MTF curves for the three rays traced through the system. At 30 cycles/mm the maximum MTF value is approximately 0.68 and the minimum is 0.53. At 50 cycles/mm the maximum MTF value is approximately 0.44 and the minimum is 0.33. This puts the system well within the desired targets.

We can examine the aberration contributions from each lens surface in the system using the Seidel diagram shown in Fig. 8. Looking at the sum of the aberrations, most are balanced to values significantly less than the aberrations for the individual lenses in the system. We can also see that, despite being optimized for specifically, distortion is the largest aberration in the system. The value reported for the distortion from the DIMX optimization operand was 0.991%.

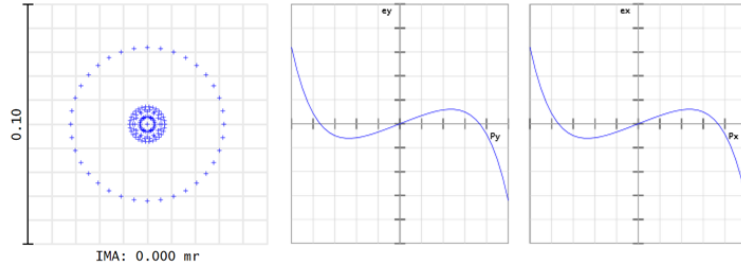


Fig. 6. Spot diagram and ray fan diagrams for the Galilean beam expander with optimal lens orientation (F-F). The units of the spot diagram are milliradians.

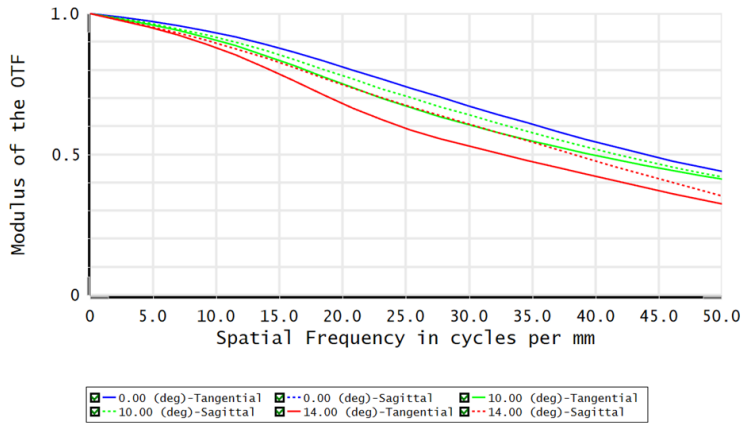


Fig. 7. Plot of the FFT MTF function for the SLR system. A tangential and sagittal curve is plotted for each of the three rays. The colors correspond to the same rays as in Fig. 3.

The last criteria was to design the system for 35 mm (24x36) film. Shown in Fig. 9 are image simulations for the system before and after optimization. The quality of the image for the optimized system is somewhat reduced from the source image. However, there is a clear improvement in the image quality from optimizing the system. The simulation reported an image size of 25.9x34.5 mm, which was close to the intended film size.

### 3.3. Young's Double Slit

Diffraction patterns of the four apertures are shown in Fig. 10. For the default aperture, we expect the third diffraction peak at 25 mm from the center of the pattern according to Eq. 3. This is consistent with detector view (a). For the aperture with half the slit spacing we expect the extent of the pattern in the x-dimension to be halved, which is also consistent with detector view (b).

Changes to the slit width and number of slits should not change the positions of the peaks, though the justification for the latter is beyond the scope of this paper. This is consistent with detector views (c) and (d). Detector view (c) shows no apparent change from the default aperture, while the spots in detector view (d) appear slightly more defined.

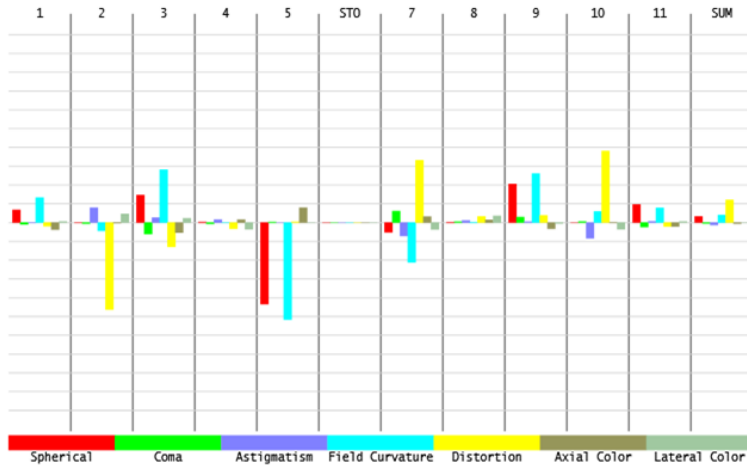


Fig. 8. Seidel diagram for the aberrations present in the SLR lens system. The rightmost column shows the sum of the aberrations for the individual surfaces.



Fig. 9. Comparison of image simulations before and after optimizing the SLR system.  
 (a) The source image for the simulation  
 (b) The simulated image after optimization  
 (c) The simulated image before optimization but after modifying parameters from the Double Gauss sample file.

### 3.4. Singlet Lenses with Zemax API

Radii and effective focal lengths of the three singlet lenses are given in Table 2. Despite having identical theoretical powers calculated from Eq. 4, there is variation in the effective focal lengths.

	Plano-Convex	Double Convex	Concave-Convex
<b>Front Radius (mm)</b>	100	200	100
<b>Back Radius (mm)</b>	Infinity	200	50
<b>EFL (mm)</b>	193.5	195.2	181.2

Table 2. Radii for the front and back surfaces of each singlet lens reported as absolute magnitudes. Also reported are the effective focal lengths for each system.

If we examine the ray traces in Fig. 11, both the plano-convex and double-convex lenses have good focus at nearly the same point on the optical axis. The best focus of the concave-convex lens, however, is poor and is shifted roughly 10 mm along the optical axis. Spot diagrams in Fig. 12 confirm that the concave-convex lens suffers from aberrations on a scale an order of magnitude larger than the other two lenses.

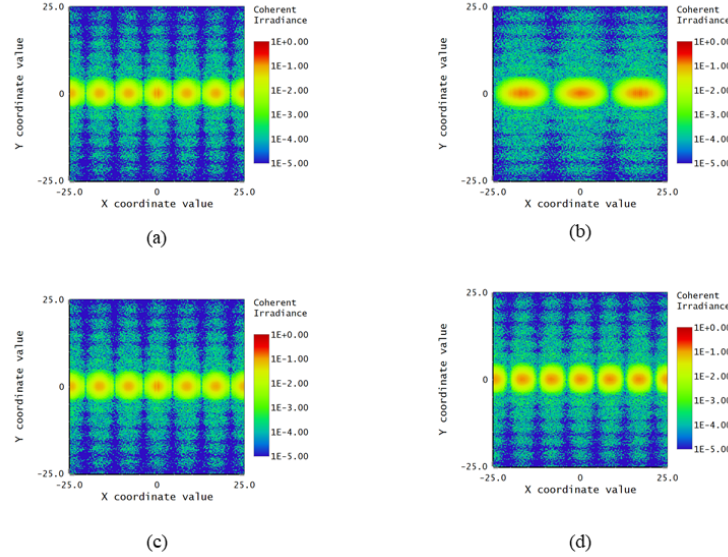


Fig. 10. Detector views of the coherent irradiance of the diffraction patterns for the default aperture (a), the aperture with  $d = 0.48$  mm (b), the aperture with  $a = 0.005$  mm (c), and the 4-slit aperture (d).

## 4. Conclusion

### 4.1. Afocal Beam Expanders

The optimal lens orientation for the Keplerian beam expander was C-F while the optimal lens orientation for the Galilean beam expander was F-F. Between the two optimal configurations the Galilean system showed a much better beam quality value. However, the F-F Galilean system showed greater deviation from the desired expansion than the C-F Keplerian system. It appears there are trade-offs between the two.

A note should be made on the choice to model the Gaussian laser beam as a bundle of collimated rays. The adequacy of this choice for the Keplerian beam expander was strained given the additional distances before and after the lens system. These distances put the system outside of the Rayleigh range of the modeled HeNe laser. The beam propagation model should be reviewed to determine if this is a significant detriment to the accuracy of the results.

### 4.2. SLR Camera

Desired MTF targets for the SLR camera lens system were comfortably exceeded. Distortion was the largest aberration in the system according to the Seidel diagram, but was kept below the maximum of 1% as measured by the DIMX operand.

More analysis should be made on the image size of the system. Running an image simulation produced dimensions close to the desired film size, but there were small differences. It is possible the incident ray angles need to be modified to ensure the system is being optimized for the correct image dimensions.

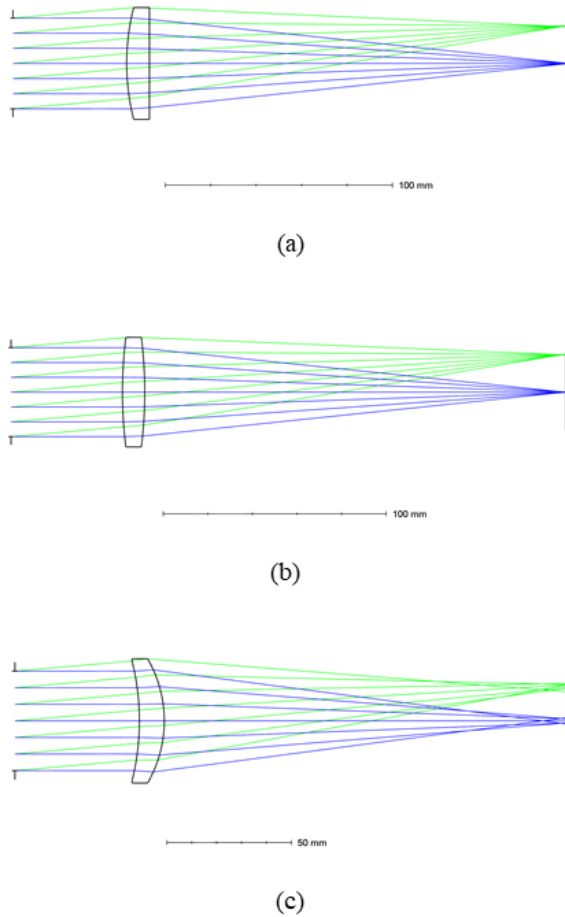


Fig. 11. Ray traces showing the focus for each lens: (a) plano-convex, (b) double convex, (c) concave-convex.

#### 4.3. Young's Double Slit

Simulation results are consistent with the predicted diffraction peak positions from Eq. 2. The simulations also showed the slit width and number of slits do not seem to have an effect on the positions of the diffraction peaks.

Additional investigations could be made into the effects of changing the wavelength and the slit-to-screen distance. There is also room to explore the impacts of the slit width and number of slits on the diffraction pattern shape in more detail.

#### 4.4. Singlet Lenses with Zemax API

Each singlet lens had a different effective focal length, despite having identical theoretical powers given by Eq. 4. The plano-convex and double convex lens had similar quality in their foci, while the focus of the concave-convex lens was significantly worse.

Much could be done to further exploit the advantages of the OpticStudio API. The lenses could be created sequentially within the same C# file while also automating the analysis procedure. This would allow exploring a large number of other lens configurations efficiently while potentially exploring the affects of other parameters.

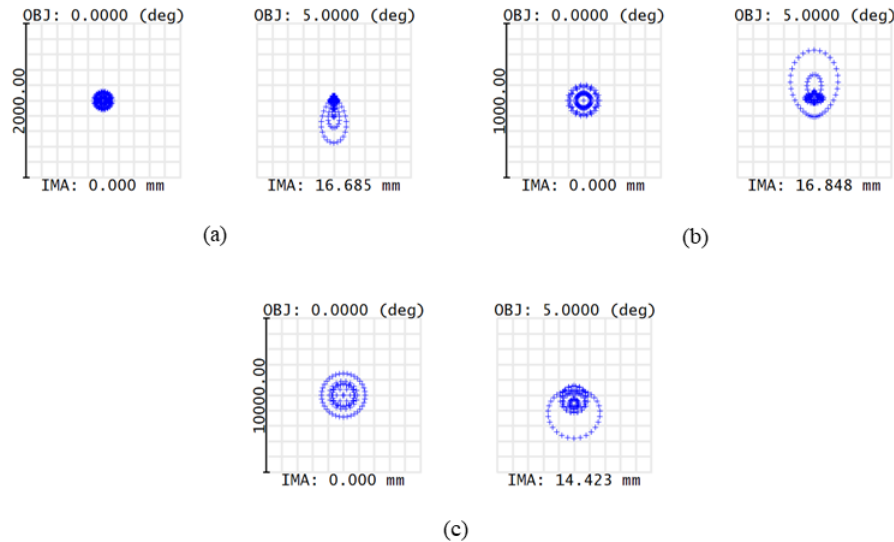


Fig. 12. Spot diagrams for both fields of the plano-convex lens (a), double convex lens (b), and concave-convex lens (c).

#### 4.5. Summary

Zemax OpticStudio is a powerful tool for modeling optical systems. Between its sequential and nonsequential modes, it has the flexibility to simulate a wide range of optical phenomena. This flexibility and the relative ease of performing optimizations and analysis make it a convenient aid in designing devices or experiments.

#### References

1. A. Arora, “Exploring non-sequential mode in opticstudio,” (March 30, 2021). Retrieved from <https://support.zemax.com/hc/en-us/articles/1500005487761-Exploring-Non-Sequential-Mode-in-OpticStudio>.
2. M. Nicholson, “How to design afocal systems,” (March 31, 2021). Retrieved from <https://support.zemax.com/hc/en-us/articles/1500005488001-How-to-design-afocal-systems>.
3. A. E. Siegman, “How to (maybe) measure laser beam quality,” in *DPSS (Diode Pumped Solid State) Lasers: Applications and Issues*, (Optical Society of America, 1998), p. MQ1.
4. H. Chen, “How to model laser beam propagation in opticstudio: Part 1 - gaussian beam theory and ray-based approach,” (March 31, 2021). Retrieved from <https://support.zemax.com/hc/en-us/articles/1500005490261-How-to-model-laser-beam-propagation-in-OpticStudio-Part-1-Gaussian-beam-theory-and-ray-based-approach>.
5. “Single-lens reflex camera,” (November 7, 2021). Retrieved from Wikipedia on November 10, 2021.
6. D. Hill, “How to design a singlet lens, part 1: Setup,” (March 30, 2021). Retrieved from <https://support.zemax.com/hc/en-us/articles/1500005576302-How-to-design-a-singlet-lens-Part-1-Setup>.
7. M. Nicholson, “Methods for analyzing mtf in opticstudio,” (March 31, 2021). Retrieved from <https://support.zemax.com/hc/en-us/articles/1500005575102-Methods-for-analyzing-MTF-in-OpticStudio>.
8. R. Poolman, “The source diffractive object,” (March 31, 2021). Retrieved from <https://support.zemax.com/hc/en-us/articles/1500005575862-The-Source-Diffractive-object>.
9. “Lens-maker’s formula,” Retrieved from <http://hyperphysics.phy-astr.gsu.edu/hbase/geoopt/lenmak.html>.
10. Thorlabs, “Hnl series red hene laser system,” (August 21, 2018). Retrieved from <https://www.thorlabs.com/thorproduct.cfm?partnumber=HNL100LB>.
11. K. Niall, “Using zos-api with c# and c++: what to install,” (March 31, 2021). Retrieved from <https://support.zemax.com/hc/en-us/articles/1500005577882-Using-ZOS-API-with-C-and-C-what-to-install>.
12. H. Gross, ed., *Handbook of Optical Systems, Volume 1: Fundamentals of Technical Optics* (Wiley, 2005).